Journal of Clinical & Experimental Ophthalmology

Echevarria et al., J Clin Exp Ophthalmol 2013, 4:3
DOI: 10.4172/2155-9570.1000286

Research Article Open Access

Stressor-dependent Alterations in Glycoprotein 130: Implications for Glial Cell Reactivity, Cytokine Signaling and Ganglion Cell Health in Glaucoma

Echevarria FD[1,2], Walker CC[2], Abella SK[2], Won M[2] and Sappington RM[2,3]

[1]Neuroscience Graduate Program, Vanderbilt University School of Medicine, 11425 Medical Research Building IV, Nashville, TN 37232-0654, USA
[2]Department of Ophthalmology and Visual Sciences (Vanderbilt Eye Institute), Vanderbilt University School of Medicine, 11425 Medical Research Building IV, Nashville, TN 37232-0654, USA
[3]Department of Pharmacology, Vanderbilt University School of Medicine, 11425 Medical Research Building IV, Nashville, TN 37232-0654, USA

Abstract

Objective: The interleukin-6 (IL-6) family of cytokines is associated with retinal ganglion cell (RGC) survival and glial reactivity in glaucoma. The purpose of this study was to evaluate glaucoma-related changes in glycoprotein-130 (gp130), the common signal transducer of the IL-6 family of cytokines, as they relate to RGC health, glial reactivity and expression of IL-6 cytokine family members.

Methods: For all experiments, we examined healthy retina (young C57), aged retina (aged C57), retina predisposed to glaucoma (young DBA/2) and retina with IOP-induced glaucoma (aged DBA/2). We determined retinal gene expression of gp130 and IL-6 family members, using quantitative PCR, and protein expression of gp130, using multiplex ELISA. For protein localization and cell-specific expression, we performed co-immunolabeling for gp130 and cell type -specific markers. We used quantitative microscopy to measure layer-specific expression of gp130 and its relationships to astrocyte and Müller glia reactivity and RGC axonal transport, as determined by uptake and transport of cholera toxin β-subunit (CTB).

Results: Gene expression of gp130 was elevated with all glaucoma-related stressors, but only normal aging increased protein levels. In healthy retina, gp130 localized primarily to the inner retina, where it was expressed by astrocytes, Müller cells and RGCs. Layer-specific analysis of gp130 expression revealed increased expression in aging retina and decreased expression in glaucomatous retina that was eccentricity-dependent. These glaucoma-related changes in gp130 expression correlated with the level of GFAP and glutamine synthetase expression, as well as axonal transport in RGCs. The relationships between gp130, glial reactivity and RGC health could impact signaling by many IL-6 family cytokines, which exhibited overall increased expression in a stressor-dependent manner.

Conclusions: Glaucoma-related stressors, including normal aging, glaucoma predisposition and IOP-induced glaucoma, differentially alter expression of gp130 and these alterations have direct implications for astrocyte and Müller glia reactivity, RGC health and cytokine signaling.

Keywords: Cytokine; Interleukin-6; Astrocyte; Müller cell; Retinal ganglion cell; Glaucoma; gp130; Glia

Introduction

Glaucoma is a neurodegenerative disease that is defined by the progressive loss of retinal ganglion cells (RGCs) and their axons, which comprise the optic nerve [1,2]. It is currently the second leading cause of irreversible blindness in the world and it is projected that over 56 million people will develop the disease by 2020 [3]. Two major risk factors associated with glaucoma are age and increased sensitivity to intraocular pressure (IOP), with the latter being the only modifiable risk factor [4].

Previous research indicates that inflammatory responses in the retina, including glial cell activation and production of inflammatory cytokines [5-18], play a role in glaucomatous degeneration of RGCs. These inflammatory responses can be either detrimental or neuroprotective for RGCs challenged by glaucomatous stressors. We and others have shown that the pro-inflammatory cytokine interleukin-6 (IL-6) is produced by retinal microglia in response to elevated IOP and may serve to protect RGCs from pressure-induced apoptosis [12,15,16]. Furthermore, IL-6 signaling varies spatially across the glaucomatous retina, suggesting a high degree of cellular regulation [19].

IL-6 is part of a group of cytokines known as the IL-6 family of cytokines and they are involved in the regulation of downstream transcription of pro- and anti- apoptotic factors. The IL-6 family of cytokines includes: IL-6, interleukin-11 (IL-11), ciliary neurotrophic factor (CNTF), leukemia inhibitory factor (LIF), oncostatin M (OSM), cardiotrophin-1 (CTF-1), cardiotropin-2 (CTF-2) and cardiotrophin-like cytokine factor-1 (CLCF1). To mediate gene transcription, IL-6 family members bind to their own specific receptor (e.g. IL-6 binds to IL-6Rα). This ligand/receptor complex then recruits glycoprotein 130 (gp130), a signal transduction receptor that is utilized by all IL-6 family members [20-22]. Once the entire signal complex is formed, gp130 is activated and initiates a variety of signal cascades that mediate transcription of pro- and anti- inflammatory factors [23-25]. Previously, our group has shown that glaucomatous neurodegeneration alters

***Corresponding author:** Rebecca M. Sappington, PhD, Department of Ophthalmology and Visual Sciences (Vanderbilt Eye Institute), Vanderbilt University School of Medicine, 11425 Medical Research Building IV, Nashville, TN 37232-0654, USA, Tel: (615) 322-0790; Fax: (615) 936-6410; E-mail: rebecca.m.sappington@vanderbilt.edu

Received May 20, 2013; **Accepted** June 27, 2013; **Published** June 30, 2013

Citation: Echevarria FD, Walker CC, Abella SK, Won M, Sappington RM (2013) Stressor-dependent Alterations in Glycoprotein 130: Implications for Glial Cell Reactivity, Cytokine Signaling and Ganglion Cell Health in Glaucoma. J Clin Exp Ophthalmol 4: 286. doi:10.4172/2155-9570.1000286

the expression and localization patterns of IL-6 and IL-6Rα in whole retina as well as in the ganglion cell and nerve fiber layers, specifically. However, little is known how glaucomatous insults affect the dynamics of gp130 expression and co-localization and how these changes related to RGC health, glial reactivity and expression of the IL-6 family of cytokines. In the current study, we assessed expression and localization gp130 and correlated changes in expression/localization with RGC function, glial reactivity and expression of IL-6 family members in response to glaucomatous neurodegeneration, as well as in the presence of two glaucoma-related stressors: aging and genetic predisposition for glaucoma. We found that normal aging increased whole retina gp130 gene expression in response to glaucomatous stressors. However, only normal aging induced detectable increases in whole retina levels of gp130 protein. In healthy retina, gp130 localized primarily to the inner retina, where it was expressed by astrocytes, Müller cells and RGCs and was expressed in an eccentricity-dependent manner. Increased gp130 expression in the ganglion cell and nerve fiber layers was at least partially responsible for changes in whole retina expression. Analysis of gp130 in whole-mounted retina demonstrated that changes in gp130 expression induced by glaucomatous stressors are accompanied by changes in GFAP and glutamine synthetase expression as well as uptake and axonal transport capacity of RGCs. Finally, stressor-dependent changes in gp130 were likewise, accompanied by overall elevated expression of IL-6 family cytokines that was also stressor-dependent in nature.

Materials and Methods

Animal and IOP data

This study was conducted in accordance to regulations set forth in the ARVO Statement for the Use of Animals in Ophthalmic and Vision Research. The Institutional Animal Care and Use Committee of Vanderbilt University Medical Center approved animal protocols. Male DBA2/J and C57BL/6 mice were obtained at 2 months and 6 months of age from Charles River Laboratories (Wilmington, MA). In DBA/2J mice, IOP was measured monthly (5-10 measurements per eye) using a tonometer (ICare Tonolab; Franconia, NH or Tono-Pen; Reichert, Depew, NY). Mice were sacrificed for experiments at either 4 months or 8 months of age.

Tissue harvest and preparation

For analysis using paraffin-embedded and whole mount retinas, C57BL/6 and DBA/2J mice were perfused with 4% paraformaldehyde (PFA; Electron Microscopy Sciences, Hatfield, PA). Whole eyes were enucleated and post-fixed for at least an hour in 4% PFA and then stored at 4 degrees celsius in 1X PBS and 0.02% sodium azide (Sigma Aldrich, St. Louis, MO) until use. 48 hours before sacrifice, mice designated for whole mount retina analysis were given a 2ul intravitreal injection of CTB conjugated to Alexa Fluor-594 (Life Technologies, Grand Island, NY) in each eye. For whole mount analysis, the retina was dissected from the eye cup, stained with toluene blue for vitreous removal and left in 1x PBS with 0.02% sodium azide until use. For paraffin retina sections, eyes were subjecting to paraffin embedding as previously described [26] and 6 µm serial sections of the entire eye were obtained. To obtain fresh retinal tissue, mice were sacrificed by cervical dislocation and whole eyes were enucleated and flash frozen on dry ice. Samples were stored at -80°C until protein or RNA isolation.

gp130 protein quantification using Luminex MAP technology

To quantify total gp130 protein concentration in young and aged DBA/2J and their C57 controls, n=5 within each experimental group were pooled and n=8 pools were analyzed per group. Transmembrane and cytosolic protein fractions were isolated using ProteoExtract Transmembrane Protein Extraction Kit (Cat. # 71772-3, EMD Millipore, Billerica, MD). Protein fractions were submitted to the Vanderbilt University Medical Center Core Laboratory for Cardiovascular and Clinical Research to determine gp130 protein concentration using the MilliPlex MAP cytokine/chemokine immunoassay kit (Cat # MSCRMAG-42K, EMD Millipore632), per manufacturer's instruction.

Quantitative Real-time polymerase chain reaction

Total RNA was isolated from young C57 (n=4), young DBA/2 (n=3), aged C57 (n=3) and aged DBA/2 (n=3), retinas using Trizol (Life Technologies), as previously described [16]. Total RNA was submitted to the Vanderbilt University Medical Center Genome Sciences Resource Microarray Core where QC/QA (quality control/quantity assessment) analysis was performed in order to ensure RNA integrity. Briefly, 1-2µl of RNA was used to measure concentration by spectrophotometry (NanoDrop 2000, Wilmington, DE) and its integrity was determined using an Agilent Bioanalyzer 2100 (Agilent Technologies, Inc., Santa Clara, CA). To pass the QC/QA analysis and be used for quantitative real-time PCR (qPCR), samples required 28S:18S ratios >0.9 and RNA integrity values >7. After quality assurance, reverse transcription of 10ng of RNA was done to generate cDNA using SuperScript II Reverse Transcriptase (Life Technologies) and Stratagene 100 mM dNTP Mix (Agilent). To assure cDNA quality, a cDNA clean-up was completed after synthesis using Agencourt Ampure XP PCR Purification kit, according to manufacturer's instructions (Beckman Coulter, Indianapolis, IN). Probe efficiency and levels of specific mRNA transcripts were assessed using Taqman Gene Expression Master Mix (Applied Biosystems, Forest City, CA) and 1 µM of TaqMan probes specific for: *gp130* (Catalog# Mm00439665_m1); *IL-11* (Mm00434162_m1); *CNTF* (Catalog# Mm00446373_m1); *LIF* (Catalog# Mm00434762_g1); *OSM* (Catalog# Mm01193966_m1); *Clcf1* (Catalog# Mm01236492_m1); *Ctf1* (Catalog# Mm00432772_m1), *Ctf2* (Catalog# Mm01701681_m1) and glyceraldehyde 3-phosphate dehydrogenase (*Gapdh*; Catalog# Mm99999915_g1) on a 7900HT Fast Real-time PCR System in triplicate (Applied Biosystems). As indicated by probe efficiencies, the ΔCt method was used to determine expression in each group (SDS software; Applied Biosystems). To calculate ΔCt, the threshold of cycle (Ct) values for each gene (gp130, IL-11, CNTF, LIF, CLCF1, OSM, Ctf1 & Ctf2) were substracted by the Ct values for the control gene GAPDH in each sample. Changes in gene expression, as compared to 4-month C57 retina, were calculated using the ΔΔCt method.

Immunohistochemistry

Paraffin whole eye sections: To evaluate the expression of gp130 against cell type markers glial fibrillary acidic protein (GFAP; astrocytes) and glutamine synthetase (GS; Müller glia), immunohistochemistry (IHC) was done on longitudinal paraffin-embedded retina sections from 4 month DBA2/J (n=6), 8 month DBA2/J (n=6) and their age matched controls (C57B6/J) (n=6 each). Sections were deparaffinized at 60°C for 1 hour followed by xylene and rehydrating ethanol series. To quench autofluorescence, sections were treated with 0.1% sodium borohydride (Fisher Scientific) for 30 minutes at room temperature. Following PBS washes, sections were incubated in a solution containing 5% normal horse serum (NHS; Life Technologies) and 0.1% Triton X-100 (Fisher Scientific) in PBS with 0.02% sodium azide for 2 hours at room temperature. Sections were incubated overnight at 4°C in a solution containing primary antibody(s), 3% NHS, and 0.1%

Triton X-100 in 1X PBS with 0.02% sodium azide. Primary antibodies used include rat anti-gp130 (1:12.5; Cat.# MAB4681,R&D Systems) rabbit anti-GFAP (1:1000; Cat.# Z-0334, DAKO), goat anti-Glutamine Synthetase (1:250; Cat.# sc-6640, Santa Cruz) and rabbit anti-β-Tubulin III (1:200; Cat.# MRB-435P, Covance). Following PBS washes, sections were then incubated for 2 hours at room temperature with the appropriate secondary antibody solution containing 1% NHS, 0.1% Triton X-100 and secondary antibody at a 1:200 concentration in 1X PBS with 0.02% sodium azide. The following secondary antibodies were used: 488-donkey anti-rat (gp130), 647-donkey anti-goat (glutamine synthetase), and Rd-Red-donkey anti-rabbit (GFAP or β-Tubulin III) (JacksonImmuno, West Grove, PA). Sections were counterstained with DAPI (1:100; Invitrogen) and coverslipped with aqueous mounting media (Southern Biotech; Birmingham, AL).

Quantification of Layer-specific immunolabeling from paraffin sections: To evaluate gp130, GFAP, Glutamine Synthesis and β-Tubulin III layer specific expression, 40x images were taken using a Roper Scientific black and white camera (Photometrics, Tucson, AZ) mounted to a Nikon Ti microscope (Nikon Instruments, Melville, NY). Regions of interest were outlined around ganglion cell and nerve fiber layers (GCL/NFL) using NIS Elements Software (Nikon) and from those regions of interest, mean intensity per area (Arbitrary Units/mm2) was measured.

Whole mount retina: For whole mount retina analyses, retinas from young C57 (n=3), aged C57 (n =3), young DBA/2 (n=3) and aged DBA/2 (n=3) from each experimental group were bisected and subjected to IHC as previously described [12,27]. One half of each retina was incubated in a solution containing primary antibodies specific for rat anti-gp130 (1:12.5; Cat.# MAB4681,R&D Systems) and goat anti-Glutamine Synthetase (1:250; Cat.# sc-6640, Santa Cruz) or anti-gp130 and rabbit anti-GFAP (1:1000; Cat.# Z-0334, DAKO). Following washes, retina were incubated in a secondary antibody solution containing either 488-donkey anti-rat (gp130; 1:200) and 647-donkey anti-goat (glutamine synthetase; 1:200) or 488-donkey anti-rat (gp130; 1:200) and Rd-Red-donkey anti-rabbit (GFAP; 1:2000). Retinas were then mounted on slides and coverslipped with aqueous mounting media (Southern Biotech).

Quantification of whole retina immunolabeling: Whole mount retina were visualized using fluorescent confocal microscopy (Olympus, Center Valley, PA) at the Vanderbilt University Cell Imaging Core. Three dimensional z-series images of the retina were acquired using a digital camera and image analysis software (FV-10 ASW; Olympus). For each retinal hemisphere, 5 pseudorandom images through the ganglion cell and nerve fiber layers of mid-peripheral to mid-central retina were obtained at 60x magnification. For each of the 5 pseudorandom retinal images the ganglion cell- and nerve fiber- layers were collapsed into two dimensional images. Intensity of CTB tracing and gp130, GFAP and glutamine synthetase immunolabeling was calculated as the mean pixel intensity across each image in arbitrary units. All measurements were performed using imaging analysis software (Image J, National Institutes of Health).

Statistical analysis

All statistical tests were performed with SigmaPlot (Systat Software Inc., San Jose, CA). Experimental groups were compared with either a one-way ANOVA or ANOVA on ranks with pairwise comparisons by Kruskal-Wallace, Student-Newman-Keuls or Dunn's post-hoc analyses. All data is presented as the mean ± standard deviation. For all analyses, $p \leq 0.05$ was considered statistically significant.

Results

Gp130 mRNA and protein expression are differentially altered by glaucoma and glaucoma-related stressors

The DBA/2 mouse contains mutations in two genes, gpnmb and tyrp1, that cause age-related atrophy and dispersion of pigmented cells from the iris [28,29]. This iris pathology leads to age-related elevation in IOP via blockade of aqueous outflow channels in the anterior segment [30,31]. The inherited and age-related aspects of glaucomatous pathology in the DBA/2 mouse are not only relevant to human forms of glaucoma, but also present the opportunity to examine genetic predisposition to glaucoma in young DBA/2 mice. We used this unique feature of the model to establish four experimental groups of age-matched C57 and DBA/2 mice: healthy retina (young C57Bl/6), aging retina (aged C57Bl/6), retina genetically predisposed to glaucoma (young DBA/2) and glaucomatous retina (aged DBA/2).

We began our assessment of gp130 expression with whole retina analysis of gp130 mRNA and protein levels. Using quantitative PCR, we found that gp130 expression increased by 45 - 60% relative to young C57 retina ($p<0.05$ for all; Figure 1A). Gene expression of gp130 was

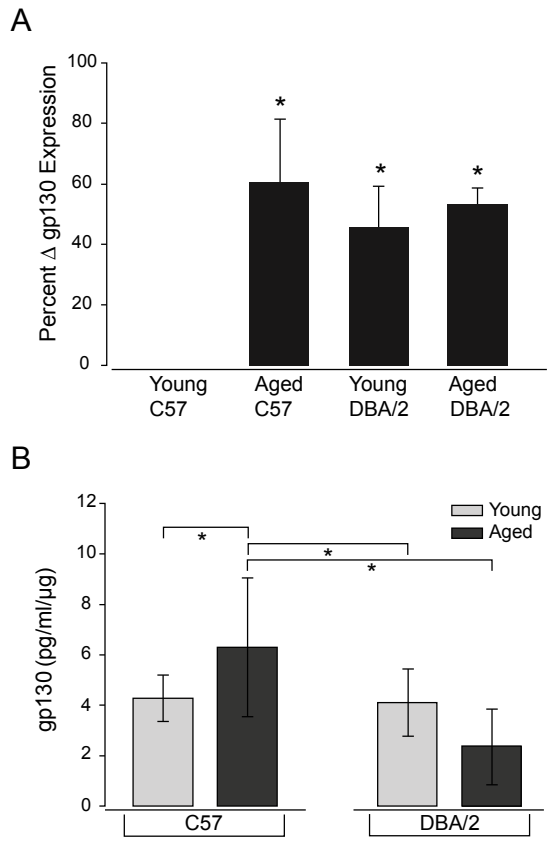

Figure 1: Stressor-dependent gene and protein expression of gp130 in whole retina. A. Gene expression of gp130 in whole retina from young C57, aged C57, young DBA/2 and aged DBA/2 mice, as determined by quantitative PCR. Levels of gene expression are determined by the delta CT method, using GAPDH as the reference gene. Data is represented as percent change in gene expression relative to expression in young C57 retina. Asterisks denote statistical significance ($p < 0.05$), as compared to expression in young C57 retina. **B.** Protein concentration of gp130 (pg/ml/μg protein) in membrane fractions of whole retina lysates from young C57, aged C57, young DBA/2 and aged DBA/2 mice, as determined by ELISA. Asterisks denote statistical significance ($p < 0.05$).

similar for aged C57, young DBA/2 and aged DBA/2 retina ($p > 0.05$; Figure 1A). For protein expression, we measured the concentration of gp130 in protein lysates, using a multi-plex ELISA assay. Since gp130 exists in both soluble and membrane-associated forms [32,33], we separated protein lysates into soluble and membrane fractions prior to ELISA analysis. In membrane fractions, gp130 protein levels were the highest in aged C57 retina (Figure 1B). The greatest disparity in gp130 protein expression was noted between aged C57 and aged DBA/2 retina, where gp130 expression was more than 2.5-fold higher in aged C57 than in aged DBA/2 retina ($p<0.05$; Figure 1B). The protein concentration of gp130 in aged C57 retina was also greater than that in young C57 and young DBA/2 retina, but only by 32% and 35%, respectively ($p >0.05$; Figure 1B). Although not statistically significant, there is also a trend towards decreased gp130 protein expression in aged DBA/2 retina, as compared to young C57 retina ($p=0.06$; Figure 1B). In soluble fractions, gp130 was undetectable in all samples. Together, these data suggest that both glaucoma and glaucoma-related stressors reduce de novo synthesis of gp130 in retina.

RGCs, astrocytes and Müller glia express gp130 in the presence and absence of glaucoma-related stressors

Next, we examined the pattern of gp130 localization, using immunohistochemistry. In whole eye paraffin sections from young C57, aged C57, young DBA/2 and aged DBA/2 retina, we examined the overall pattern of localization as well as cell type-specific expression in central and peripheral retina. Cell type-specific expression was determined by co-immunolabeling with gp130 and cell type-specific markers for RGCs (β-tubulin), astrocytes (GFAP) and Müller glia (glutamine synthetase). In healthy retina, gp130 immunolabeling was primarily observed in the inner retina, where labeling was present in the nerve fiber, ganglion cell, inner plexiform and inner nuclear layers (Figure 2). Little to no staining was observed in the outer plexiform and outer nuclear layers as well as outer segments of the photoreceptors (Figure 2). In central retina, co-immunolabeling revealed localization of gp130 to β-tubulin + RGCs (Figure 3A), GFAP + astrocytes (Figure 3B) and glutamine synthetase + Müller glia (Figure 3C), regardless of experimental group. This suggests that glaucoma and glaucoma-related stressors do not readily alter the pattern of gp130 localization in central retina. In peripheral retina, the pattern of gp130 was similar to that in central retina (Figure 4 compare to Figure 3) with no observable changes in the presence of glaucoma or glaucoma-related stressors (Figure 4). However, the intensity of gp130 labeling appeared qualitatively greater than that in central retina (Figure 4 compare to Figure 3). Interestingly, gp130 labeling in peripheral retina also appeared greater than young C57 retina, young DBA/2 retina and aged DBA/2 retina (Figure 4). This finding correlates well with the age-related increase in gp130 protein concentration noted in our whole retina ELISA analysis. These increases in gp130 labeling were coincident with β-tubulin + RGCs (Figure 4A), GFAP+ astrocytes (Figure 4B) and glutamine synthetase + Müller glia (Figure 4C), suggesting that changes in gp130 expression are due, at least in part, to increased expression by these three cell types. Together, these data suggest that glaucoma and glaucoma-related stressors do not significantly alter the overall pattern of gp130 localization in retina, but do appear to alter expression levels, particularly in peripheral retina.

Glaucoma-related changes in gp130 expression are dependent on eccentricity

To measure observed changes in gp130 expression specifically in the ganglion cell and nerve fiber layers, we quantified the intensity of immunolabeling for gp130 in central and peripheral retina from young

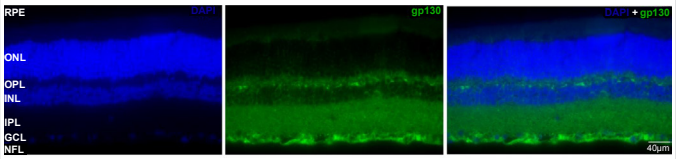

Figure 2: Constitutive expression of gp130 localizes primarily to the inner retina in healthy retina. Representative fluorescent micrographs of gp130 immunolabeling (green) with DAPI counterstain (blue) in paraffin sections of whole eye from C57 retina reveals the presence of gp130 in the OPL, INL, IPL, GCL and NFL.

RPE: Retina pigment epithelium; ONL: Outer nuclear layer; OPL: Outer plexiform layer; INL: Inner nuclear layer; IPL: Inner plexiform layer; GCL: Ganglion cell layer; NFL: Nerve fiber layer

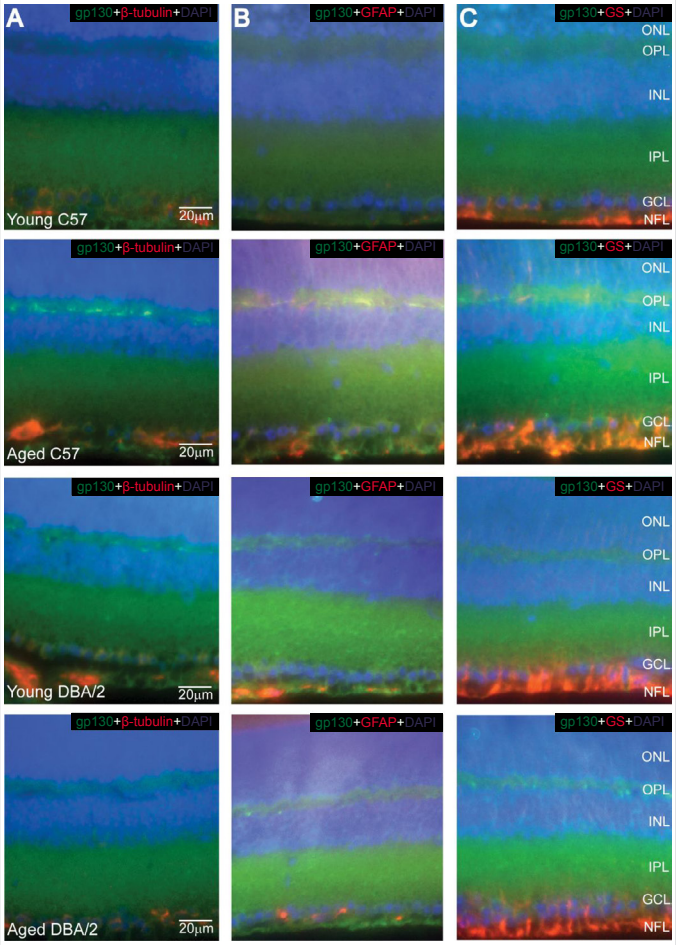

Figure 3: Glaucoma-related stressors do not alter localization of gp130 to RGCs, astrocytes and Müller glia in central retina. Representative fluorescent micrographs of central retina in whole eye paraffin sections from young C57 (top row), aged C57 (second row), young DBA/2 (third row) and aged DBA/2 (fourth row) mice. Co-immunolabeling with gp130 (green) and cell type-specific markers (red) for RGCs (β-tubulin; **A**), astrocytes (GFAP; **B**) and Müller glia (glutamine synthetase (**C**) plus DAPI counterstain (blue) reveals co-localization of gp130 (yellow) with β-tubulin, GFAP and glutamine synthetase in the GCL and NFL. Scaling is consistent for all images.
GS: Glutamine synthetase; ONL: Outer nuclear layer; OPL: Outer plexiform layer; INL: Inner nuclear layer, IPL: Inner plexiform layer; GCL: Ganglion cell layer; NFL: Nerve fiber layer

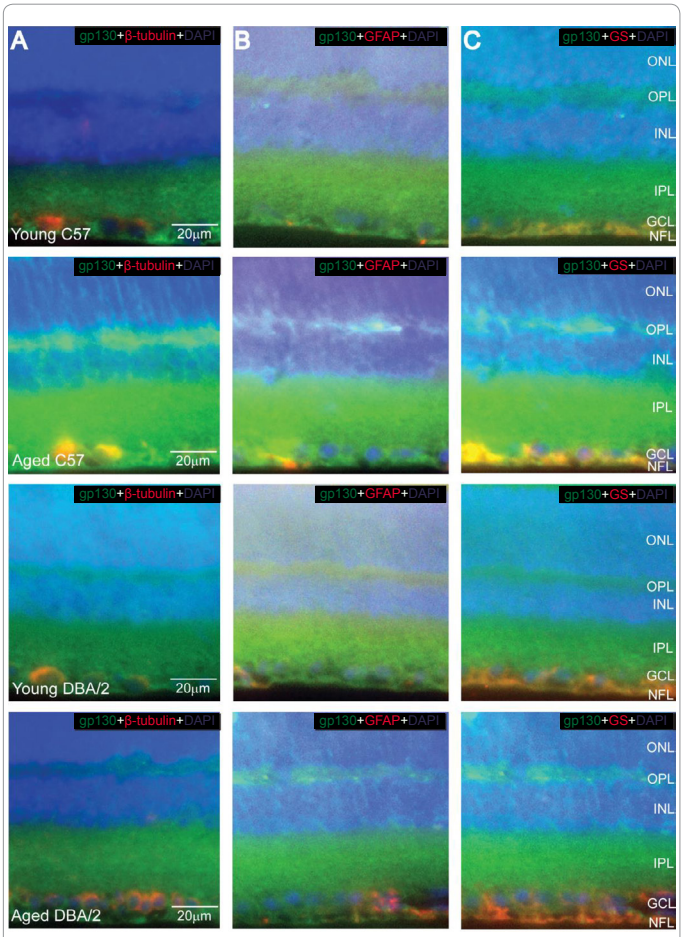

Figure 4: Glaucoma-related stressors do not alter localization of gp130 to RGCs, astrocytes and Müller glia in peripheral retina. Representative fluorescent micrographs of peripheral retina in whole eye paraffin sections from young C57 (top row), aged C57 (second row), young DBA/2 (third row) and aged DBA/2 (fourth row) mice. Co-immunolabeling with gp130 (green) and cell type-specific markers (red) for RGCs (β-tubulin; **A**), astrocytes (GFAP; **B**) and Müller glia (glutamine synthetase (**C**) plus DAPI counterstain (blue) reveals co-localization of gp130 (yellow) with β-tubulin, GFAP and glutamine synthetase in the GCL and NFL. Scaling is consistent for all images.
GS: Glutamine synthetase; ONL: Outer nuclear layer; OPL: Outer plexiform layer; INL: Inner nuclear layer; IPL: Inner plexiform layer; GCL: Ganglion cell layer; NFL: Nerve fiber layer

C57, aged C57, young DBA/2 and aged DBA/2 mice. In central retina, we found no significant difference in the intensity of gp130 labeling in the ganglion cell and nerve fiber layers between groups ($p>0.05$; Figure 5A). This suggests that both glaucoma and glaucoma-related stressors do not significantly alter gp130 expression in the ganglion cell and nerve fiber layers of central retina. The intensity of gp130 immunolabeling was greater in peripheral retina than in central retina for all groups ($p>0.05$). As suggested by our qualitative assessment of gp130 localization, the labeling intensity for gp130 in the ganglion cell and nerve fiber layers was greater in aged C57 retina than in all other groups ($p<0.05$; Figure 5B). This elevated intensity in aged C57 retina was 37%, 32% and 26% greater than young C57, young DBA/2 and aged DBA/2 retina, respectively (Figure 5B). There was no significant difference in labeling intensity of gp130 between young C57, young DBA/2 and aged DBA/2 retina ($p>0.05$; Figure 5B). Together, these data suggest that constitutive expression of gp130 expression in the ganglion cell and nerve fiber layers increases with increasing eccentricity. Interestingly, only normal aging significantly altered gp130 expression in the ganglion cell and nerve fiber layers and then, only in the peripheral retina, where constitutive gp130 expression was highest.

Stressor-dependent changes in gp130 are accompanied by alterations in glial reactivity and RGC health

To determine whether changes in gp130 expression in the ganglion cell and nerve fiber layers are related to RGC, astrocyte and Müller cell responses to glaucomatous stressors, we quantified the intensity of immunolabeling for gp130, GFAP and glutamine synthetase in whole mount retina from young and aged C57 mice and young and aged DBA/2 mice injected with the axonal tracer, cholera toxin β subunit. Previous studies indicate that uptake and anterograde transport of CTB by RGCs is an early indicator of RGC decline [34-36]. Similarly, expression of GFAP by astrocytes and glutamine synthetase by Müller cells is altered in response to retinal damage, including glaucoma [37-

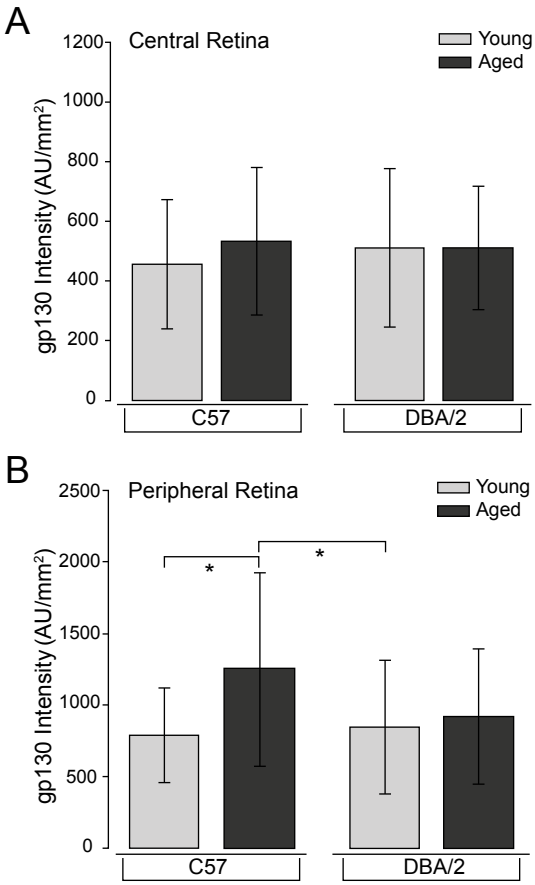

Figure 5: Expression of gp130 in the ganglion cell and nerve fiber layers is dependent upon eccentricity and increases with normal aging. Quantification of immunolabeling in the ganglion cell and nerve fiber layers of central (**A**) and peripheral (**B**) regions of retina in whole eye paraffin sections from young C57, aged C57, young DBA/2 and aged DBA/2 mice. Data is plotted as intensity of gp130 immunolabeling in arbitrary units and asterisks indicate statistical significance ($p < 0.05$). Glaucoma-related stressors do not alter the intensity of gp130 immunolabeling in central retina (**A**). The intensity of gp130 labeling is greater in peripheral retina than in central retina for all groups (**B** compare to **A**). In peripheral retina, labeling intensity of gp130 is greater in aged C57 retina than that in young C57 and DBA/2 retina (**B**).

44]. For our analysis in whole mount retina, we sampled 60x fields in the area between mid-central and mid-peripheral retina. We selected this region to achieve comparable assessment of CTB labeling in RGC soma and axons.

First, we assessed mean changes in gp130, GFAP, glutamine synthetase and CTB intensities. We found that in the mid-central to mid-peripheral retina, labeling intensity of gp130 was similar between young and aged C57 retina ($p > 0.05$; Figure 6A). This level of gp130 intensity was 24% (young DBA/2; $p=0.05$) and 33% (aged DBA/2; $p=0.01$) than in aged C57 retina (Figure 6A). Labeling intensity of gp130 was also 28% less in aged DBA/2 retina than in young C57 retina ($p=0.04$; Figure 6A). For axonal transport, we found that aged DBA/2 retina exhibited 38% ($p< 0.01$) and 18% ($p=0.04$) lower intensity of CTB labeling than aged C57 and young DBA/2 retina, respectively (Figure 6A). Interestingly, aged C57 retina exhibited CTB labeling that was 24% greater than young C57 retina ($p< 0.01$; Figure 6B). For GFAP, young C57 and DBA/2 retina ($p=0.84$) and aged C57 and DBA/2 ($p=0.53$) exhibited similar levels labeling intensity (Figure 6C). However, young exhibited labeling intensity that was 34 - 41% higher than aged retina, regardless of strain ($p<0.01$ for all; Figure 6C). For glutamine synthetase, young and aged C57 retina exhibited similar levels of labeling intensity ($p>0.05$; Figure 6D). Young and aged DBA/2 retina also exhibited similar levels of labeling intensity, but these levels were on order of 55% less than C57 retina ($p<0.05$ for all; Figure 6D). Together, these data suggest that changes in gp130 expression induced by glaucomatous stressors are accompanied by changes in GFAP expression by astrocytes, glutamine synthetase expression by Müller glia endfeet and uptake and axonal transport capacity of RGCs. Furthermore, the nature of these changes in RGC, astrocyte and Müller glia populations, like gp130 expression, are also stressor-dependent.

Stressor-dependent changes in gp130, glial reactivity and RGC health are correlative

To determine whether changes in gp130, glia reactivity and RGC health induced by glaucomatous stressors are spatially interrelated, we performed polynomial regression analyses of spatially coincident CTB labeling and gp130, GFAP and glutamine synthetase immunolabeling in whole mount retina, as described above. We found that constitutive expression of gp130 in the ganglion cell and nerve fiber layers of young C57 mice was highly correlated to intensity of CTB, GFAP and glutamine synthetase labeling (Figure 7). Specifically, CTB ($r2=0.40$, $p<0.01$; Figure 7A), GFAP ($r2=0.66$, $p<0.01$; Figure 7B) and glutamine synthetase ($r2=0.82$, $p<0.01$; Figure 7C) all reliably predicted gp130 labeling intensity in a first-order, linear relationship, where higher levels of CTB, GFAP and glutamine synthetase also exhibited higher levels of gp130 labeling. We also found that CTB labeling predicted GFAP ($r2=0.25$, $p=0.02$; Figure 8A) and glutamine synthetase ($r2=0.32$, $p<0.01$; Figure 8B) intensities via first-order, linear relationships, where areas with higher levels of CTB labeling also exhibited higher levels of GFAP and glutamine synthetase labeling (Figure 8). In these healthy retina, lower and higher values for CTB, GFAP and glutamine synthetase were related to eccentricity, where lower values were obtained in images from mid-peripheral regions, which have lower RGC density, smaller axon bundles and correspondingly, less dense populations of astrocytes and Müller glia than mid-central regions (Figures 7 and 8, right panels). These data suggest that expression of gp130 reflects the anatomical organization of healthy retina and is related to the density of RGCs, astrocytes and Müller glia.

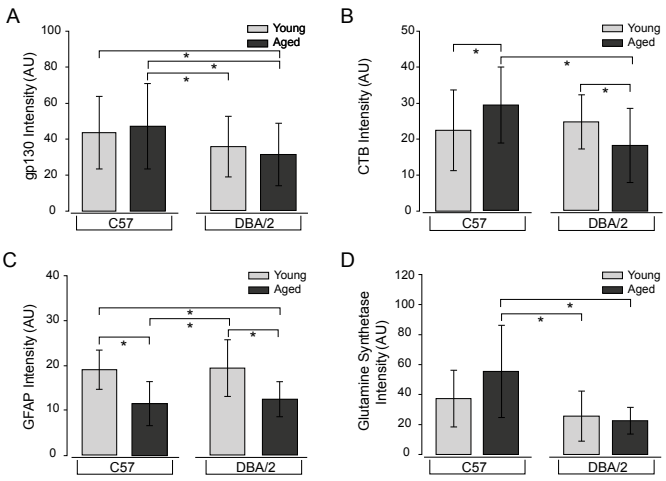

Figure 6: Glaucoma-related stressors differentially alter RGC axonal transport and expression of gp130, GFAP and glutamine synthetase in the ganglion cell and nerve fibers of mid retina. Quantification of fluorescent intensity for cholera toxin-β (CTB) uptake/transport and immunolabeling against gp130 (**B**), GFAP (**C**) and glutamine synthetase (**D**) in the ganglion cell and nerve fiber layers of mid-central to mid-peripheral regions of wholemounted retina from young C57, aged C57, young DBA/2 and aged DBA/2 mice . Data is plotted as intensity of CTB or immunolabeling in arbitrary units. Asterisks indicate statistical significance ($p < 0.05$).

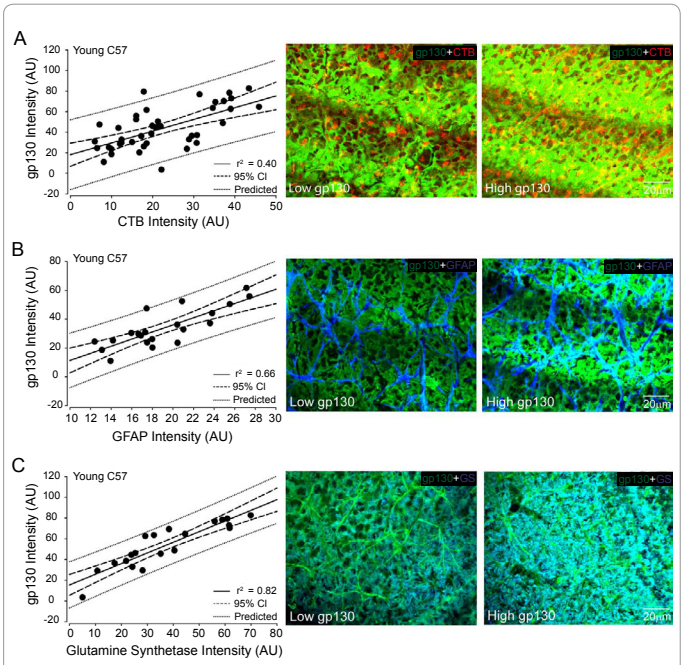

Figure 7: Constitutive expression of gp130 correlates with axonal transport in RGCs and GFAP and glutamine synthetase expression by astrocytes and Muller glia, respectively. Left panels: Regression graphs of fluorescent intensity for gp130 immunolabeling and intensity of cholera toxin-β (CTB) uptake/transport (**A**), GFAP immunolabeling (**B**) and glutamine synthetase (GS; **C**) immunolabeling in the ganglion cell and nerve fiber layers of mid-central to mid-peripheral regions of wholemounted retina from young C57 mice. Data is plotted as intensity of gp130 (y-axis) versus intensity of CTB (**A**; x-axis), GFAP (**B**; x-axis) or GS (**C**; x-axis) in arbitrary units. Solid line indicates regression line based on r2 value. Dashed line indicates the 95% confidence interval. Dotted line indicates predicted values based on r2 and 95% confidence. **Right panels:** Representative confocal micrographs depicting relationships between gp130 immunolabeling (green) and CTB transport (red; **A**), GFAP (blue; **B**), and GS (blue; **C**) labeling. For all, examples of low (left) and high (right) intensities are provided. Scaling is consistent for all images.

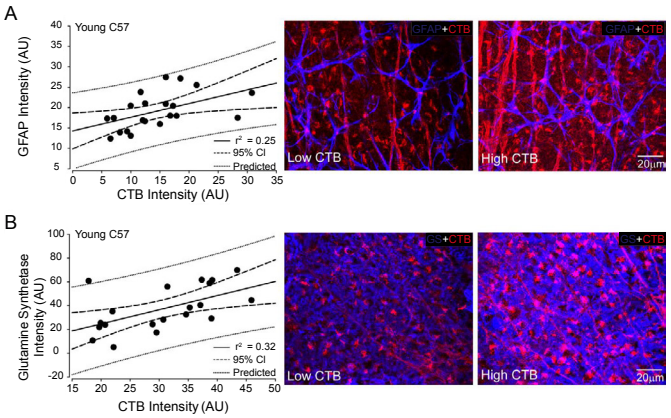

Figure 8: Axonal transport in RGCs correlates with GFAP and glutamine synthetase expression in healthy retina. Left panels: Regression graphs of fluorescent intensity for GFAP (**A**) and glutamine synthetase (GS; **B**) immunolabeling as a function of cholera toxin-β (CTB) uptake/transport in the ganglion cell and nerve fiber layers of mid-central to mid-peripheral regions of whole mounted retina from young C57 mice. Data is plotted as intensity of GFAP (y-axis; **A**) and glutamine synthetase (y-axis; **B**) versus intensity of CTB (x-axis) in arbitrary units. Solid line indicates regression line based on r2 value. Dashed line indicates the 95% confidence interval. Dotted line indicates predicted values based on r2 and 95% confidence. **Right panels:** Representative confocal micrographs depicting relationships between CTB transport (red) and GFAP (blue; **A**), and GS (blue; **B**) immunolabeling. For all, examples of low (left) and high (right) intensities are provided. Scaling is consistent for all images.

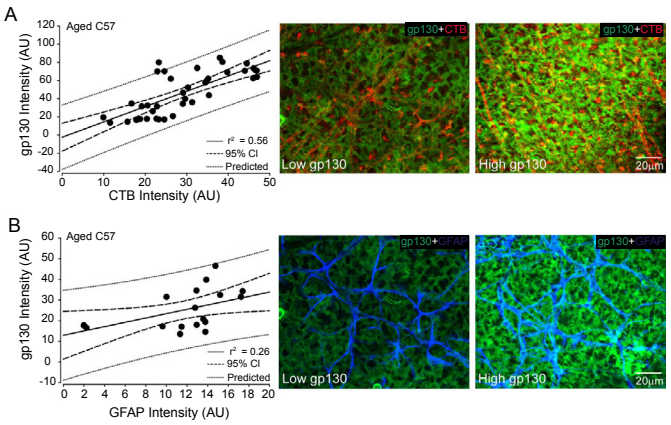

Figure 9: RGC axonal transport and GFAP expression predict gp130 expression in the ganglion cell and nerve fiber layers of aging retina. Left panels: Regression graphs of fluorescent intensity for gp130 immunolabeling and intensity of cholera toxin-β (CTB) uptake/transport (**A**) and GFAP immunolabeling (**B**) in the ganglion cell and nerve fiber layers of mid-central to mid-peripheral regions of whole mounted retina from aged C57 mice. Data is plotted as intensity of gp130 (y-axis) versus intensity of CTB (x-axis; **A**) and GFAP (x-axis; **B**) in arbitrary units. Solid line indicates regression line based on r2 value. Dashed line indicates the 95% confidence interval. Dotted line indicates predicted values based on r2 and 95% confidence. **Right panels:** Representative confocal micrographs depicting relationships between gp130 immunolabeling (green) and CTB transport (red; **A**) and GFAP immunolabeling (blue; **B**). For all, examples of low (left) and high (right) intensities are provided. Scaling is consistent for all images.

With the introduction of glaucoma-related stressors, the predictive value of gp130, glial reactivity and RGC health relationships was significantly reduced. In aged retina, gp130 labeling intensity was predicted by only CTB labeling (r2=0.56, p<0.01) and GFAP labeling (r2=0.26, p=0.03; Figure 9B). Similar to young C57 retina, these relationships were also best described by a first-order, linear regression, where areas with higher CTB and GFAP labeling also exhibited higher levels of gp130 labeling (Figure 9). However, compared to young C57 retina, the correlation between CTB intensity and gp130 intensity was greater, while the correlation between GFAP intensity and gp130 intensity was reduced (Figure 9 compare to Figure 7). While aged C57 retina retained some eccentricity effects regarding GFAP and CTB intensities, there were many instances of reduced GFAP and CTB intensity in areas of equivalent eccentricity (Figure 9, right panels). There were no other significant relationships between CTB, GFAP, glutamine synthetase and gp130 labeling by polynominal regression analysis (p > 0.05; data not shown). These data suggest that normal aging de-couples and/or weakens the spatial relationships between gp130, astrocyte and Müller glia reactivity and RGC health. Most notably, all correlations with glutamine synthetase expression were lost, suggesting that normal aging has a significant impact on Müller glia.

Like aged C57 retina, young DBA/2 retina exhibited a limited number of predictive relationships between intensities of CTB, GFAP, glutamine synthetase and gp130 labeling. However, unlike aged C57 retina, only glial reactivity correlated with gp130 expression. Both GFAP (r2=0.38, p<0.01; Figure 10A) and glutamine synthetase (r2=0.83, p<0.01; Figure 10B) reliably predicted gp130 labeling in first-order, linear relationships, where areas with higher GFAP and glutamine synthetase expression also exhibited higher levels of gp130 labeling. Interestingly, the strength of the correlation between glutamine synthetase and gp130 was similar to young C57 retina, but the strength of the correlation between GFAP and gp130 was much lower (Figure 10 compare to Figure 7). There were no other significant relationships between CTB, GFAP, glutamine synthetase and gp130 labeling by polynominal regression analysis (p>0.05; data not shown). These data suggest that a genetic predisposition to glaucoma alone

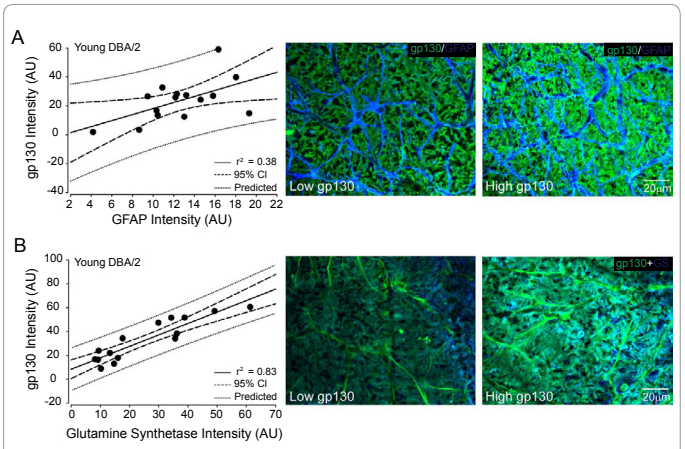

Figure 10: GFAP and glutamine synthetase expression predict gp130 expression in the ganglion cell and nerve fiber layers of retina predisposed to glaucoma. Left panels: Regression graphs of fluorescent intensity for gp130 immunolabeling and intensities of GFAP (**A**) and glutamine synthetase immunolabeling (GS; **B**) in the ganglion cell and nerve fiber layers of mid-central to mid-peripheral regions of whole mounted retina from young DBA/2 mice. Data is plotted as intensity of gp130 (y-axis) versus intensity of GFAP (x-axis; **A**) and GS (x-axis; **B**) in arbitrary units. Solid line indicates regression line based on r2 value. Dashed line indicates the 95% confidence interval. Dotted line indicates predicted values based on r2 and 95% confidence. **Right panels:** Representative confocal micrographs depicting relationships between gp130 (green) and GFAP (blue; **A**) and GS immunolabeling (blue; **B**) labeling. For all, examples of low (left) and high (right) intensities are provided. Scaling is consistent for all images.

is sufficient to alter the relationships between gp130 expression and glial cell reactivity and RGC health. It is of particular note that young DBA/2 retina, lacks spatial correlation between RGC axonal transport and gp130, GFAP and glutamine synthestase expression, suggesting that relationships between gp130 and glial cell organization are not dependent upon the density or transport capacity of RGCs.

Similar to young DBA/2 retina, GFAP labeling and glutamine synthetase labeling both predicted the intensity of gp130 labeling (Figures 11A and 11B). As with young DBA/2 retina, the first-order, linear relationships between gp130 and GFAP (r2=0.32, p=0.02; Figure 11A) and gp130 and glutamine synthetase (r2=0.66, p<0.01; Figure 11B) indicated positive correlations, where areas with higher GFAP and glutamine synthetase intensity also exhibited higher levels of gp130 labeling. The strength of these correlations was similar to that noted in young DBA/2 retina (Figure 11 compare to Figure 10). Unlike aged C57 and young DBA/2 retina, GFAP labeling was also predicted by the intensity of CTB labeling (r2=0.27, p=0.04; Figure 11C). Interestingly, this first-order, linear relationship described a negative correlation, where areas with lower CTB labeling tended to exhibit lower levels of GFAP labeling (Figure 11C). This is in contrast to young C57 retina, where a similar strength of correlation between CTB and GFAP labeling was noted, but in the positive direction (Figure 11C compare to Figure 8A). There were no other significant relationships between CTB, GFAP, glutamine synthetase and gp130 labeling by polynominal regression analysis ($p > 0.05$; data not shown). These data suggest that, like glaucoma-related stressors, glaucoma itself not only de-couples and/or weakens the constitutive relationships between gp130 expression and RGC health and glial reactivity, but can also reverse these existing relationships.

Gene expression changes in IL-6 family cytokines are also stressor-dependent

Glaucoma-related changes in IL-6 expression and signaling in retina and optic nerve have been well-documented [12,15-17,19,45,46]. To determine how stressor-dependent changes in gp130 expression may relate to signal transduction induced by other members of the IL-6 cytokine family, we measured mRNA expression of the IL-6 family members, IL-11, CNTF, LIF, OSM, CLCF1, CTF1 and CTF2, using quantitative PCR. Since we previously reported changes in IL-6 signaling in DBA/2 mice and age-matched C57 mice [12,19], we omitted IL-6 from this gene expression panel. To control for gene transcription levels, the CT for all cytokines were normalized to the CT for GAPDH (ΔCT). We found that glaucoma-related stressors tended to increase gene expression of IL-6 family members, with the exception of CTF 2, which was undetectable in all samples (Figure 12). For CNTF, LIF, CLCF1 and CTF1, aged C57, young DBA/2 and aged DBA/2 retina exhibited similar levels of gene transcription ($p > 0.05$ for all). For all stressors, gene expression increased by approximately 40% for CNTF ($p<0.01$; Figure 12A), LIF ($p<0.01$; Figure 12B) and CLCF1 ($p<0.01$; Figure 12C) and by approximately 45% for CTF1 ($p<0.01$; Figure 12D), as compared to young C57 retina. In contrast, both IL-11 and OSM exhibited stressor-dependent changes in gene expression. For OSM, young DBA/2 retina exhibited the highest level of expression, which was almost 2-fold higher than young C57 retina and approximately 60% greater than aged C57 and DBA/2 retina ($p<0.01$ for all; Figure 12E). Aged C57 and aged DBA/2 retina exhibited similar levels of expression ($p > 0.05$) that was approximately 40% greater than that of young C57 retina ($p<0.01$; Figure 12E). In contrast, aged C57 retina exhibited the highest level of IL-11 expression, which was 58% greater than young C57 retina and approximately 18% greater than young and aged DBA/2 retina ($p<0.01$ for all; Figure 12F). IL-11 expression was similar in young and aged DBA/2 retina ($p > 0.05$; Figure 12F) and this level of expression was approximately 30% greater than young C57 retina ($p<0.01$; Figure 12F). Together, these data suggest that while any glaucoma-related stressor is sufficient to elevate IL-6 cytokine family members, IL-11 and OSM, in particular appear to be stressor-dependent.

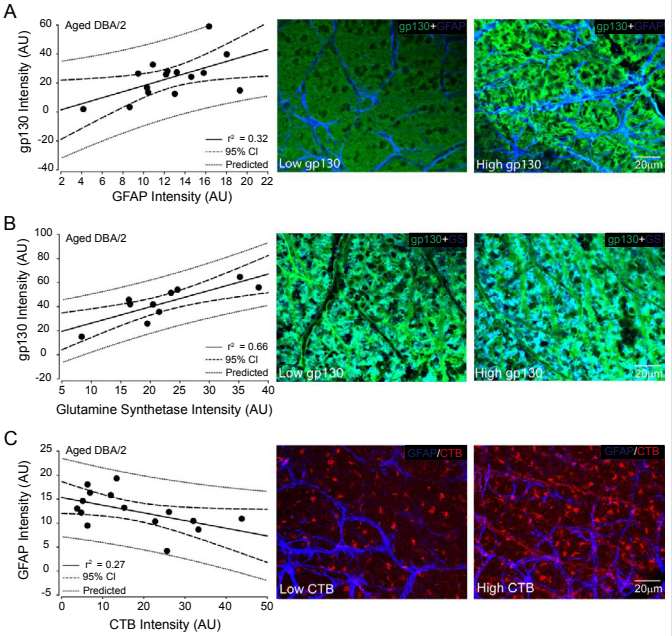

Figure 11: IOP-induced glaucoma alters the strength and nature of relationships between RGC axonal transport and expression of gp130, GFAP and glutamine synthetase. Left panels: Regression graphs of fluorescent intensity for gp130 immunolabeling and intensities of GFAP (**A**) and glutamine synthetase immunolabeling (GS; **B**) as well as fluorescent intensity of CTB labeling and GFAP immunolabeling (**C**) in the ganglion cell and nerve fiber layers of mid-central to mid-peripheral regions of wholemounted retina from aged DBA/2 mice. **A,B.** Data is plotted as intensity of gp130 (y-axis) versus intensity of GFAP (x-axis; **A**) and GS (x-axis; **B**) in arbitrary units. **C.** Data is plotted as intensity of GFAP (y-axis) versus intensity of CTB labeling (x-axis). For all, solid lines indicate regression line based on r2 value. Dashed lines indicate the 95% confidence interval. Dotted lines indicate predicted values based on r2 and 95% confidence. **Right panels:** Representative confocal micrographs depicting relationships between gp130 (green) and GFAP immunolabeling (blue; **A**), gp130 (green) and GS immunolabeling (blue; **B**) and CTB transport (red) and GFAP immunolabeling (blue, **C**). For all, examples of low (left) and high (right) intensities are provided. Scaling is consistent for all images.

Discussion

Here we described changes in expression and localization of the signal transducer gp130 in response to glaucoma-related stressors, including normal aging, genetic predisposition to glaucoma and IOP-induced glaucoma. We then correlated these alterations in gp130 with astrocyte and Müller glia reactivity, RGC health and expression of cytokines from the IL-6 family.

In healthy retina, gp130 was constitutively expressed in the membrane-bound configuration and primarily localized to the inner retina, where it is associated with RGCs, astrocytes and Müller glia. This is consistent with previous findings of gp130 localization in mouse retina [47]. Interestingly, protein expression of gp130 in the ganglion cell and nerve fiber layers, as determined by intensity of

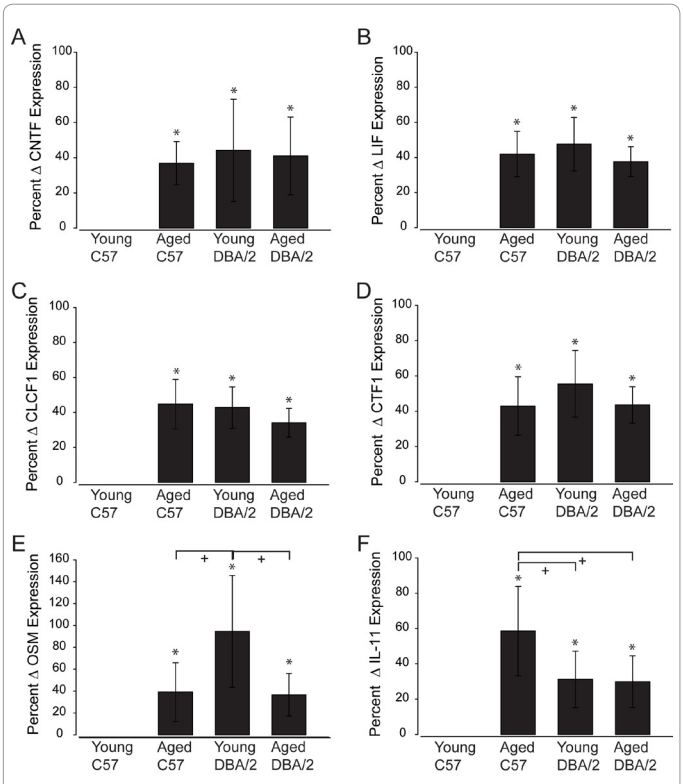

Figure 12: Glaucoma-related stressors elevate expression of IL-6 family members in a stressor-dependent manner. Gene expression of CNTF (**A**), LIF (**B**), CLCF1 (**C**), CTF1 (**D**), OSM (**E**) and IL-11 (**F**) in whole retina from young C57, aged C57, young DBA/2 and aged DBA/2 mice, as determined by quantitative PCR. Levels of gene expression are determined by the ΔΔCT method, using GAPDH as the reference gene. Data are presented as percent change in gene expression relative to expression in young C57 retina (ΔΔCT). **A-D.** Asterisks denote statistical significance ($p < 0.05$), as compared to expression in young C57 retina. **E,F.** Asterisks denote statistical significance ($p < 0.05$), as indicated by brackets.

immunolabeling, was dependent upon eccentricity, where peripheral retina exhibited higher levels of gp130 expression than central retina. This suggests a potential site-specific role for gp130-mediated signaling in peripheral retina.

In conditions of normal aging, genetic predisposition to glaucoma and IOP-induced glaucoma, mRNA levels of gp130 increased. While a corresponding increase in membrane-bound gp130 was noted in aging retina, levels of membrane-bound gp130 remained unchanged and actually trended toward decreased levels in DBA/2 mice. These discrepancies between mRNA and protein expression in response to glaucoma-specific stressors could be due to either translation or protein stability, which are both known to regulate gp130 protein levels [48-50]. Furthermore, these findings contrast with gp130 expression following acute injury in the retina, where protein expression of gp130 increases for up 48 hours after excitotoxic insult [51]. This raises the possibility that gp130-mediated signaling is induced early following acute injury, but is downregulated with chronic insults, such as IOP-induced glaucoma.

Layer-specific analysis of gp130 expression in aged C57, young DBA/2 and aged DBA/2 retina determined that glaucoma-related stressors alter gp130 expression in both stressor- and eccentricity-dependent manners. For all stressors, gp130 expression in peripheral retina was greater than that in central retina, suggesting that the constitutive functions performed by gp130-mediated signaling in the peripheral retina persist in the presence of glaucoma-related stressors. While gp130 expression appeared to be unaltered in the central retina, at least in our models and age groups, the peripheral and middle retina exhibited stressor-dependent changes in gp130 expression, which included increased expression in aging retina and decreased expression in retina with predisposition to glaucoma or IOP-induced glaucoma. These findings suggest that gp130-mediated signaling is highly regulated with the potential for discreet, site-specific functions.

Given that gp130 was primarily localized to inner retina and specifically associated with RGCs, Müller glia and astrocytes, we investigated the potential for alterations in gp130 expression to be related to both RGC health, which was measured as uptake and transport of the neural tracer CTB [34-36], and glial reactivity. As a general measure of glial reactivity, we examined immunolabeling intensity of the astrocyte marker GFAP and the Müller glia marker glutamine synthetase. An increase in the expression of these markers is associated with increased reactivity or activation of astrocytes and Müller glia in response to a variety of stressors in retina [37-44]. Since we evaluated overall labeling intensity, increases in GFAP or glutamine synthetase levels can be attributed to either increased expression on a per cell basis, which accompanies hypertrophy, or an increase in density. Both hypertrophy and changes in cell density are hallmarks of glial reactivity and have been described in various retinal diseases, including glaucoma [5,52-58]. In all groups, we noted instances of changes in expression/cell and, for astrocytes, differences in cell density. Our analyses revealed that constitutive expression of gp130 is highly correlated with RGC axonal transport, GFAP expression and glutamine synthetase, which also correlated with another. This is consistent with previous literature highlighting a role for gp130 in the survival of photoreceptors, maturation of optic nerve head astrocytes, and Müller cell activation following optic nerve lesion [59-61]. Surprisingly, normal aging, glaucoma predisposition and IOP-induced glaucoma all reduced the strength of correlations between gp130, RGC health and glia reactivity, suggesting that either gp130-mediated signaling and glial reactivity become dysregulated by glaucoma-related stressors or more likely, that regulation of these responses by other factors increases in response to stress.

To determine how alterations in gp130 expression may impact cytokine signaling, we examined gene expression of cytokines in the IL-6 family. Previous work indicates that glaucoma-related stressors alters IL-6 signaling, which is related to both glial responses and RGC health [12,15-17,19,25,51,62]. Recent work also suggests that other members of the IL-6 cytokine family, which all utilize gp130 for signal transduction, are also implicated in retinal disease, including glaucoma, diabetic retinopathy and retinal trauma [62-66]. We found that all examined members of the IL-6 cytokine family were elevated with glaucoma-related stressors, as compared to young, healthy retina. For most of these cytokines, expression levels were elevated to similar levels, suggesting an overall increase in retinal neuroinflammation. These results are consistent with previous reports of elevations in IL-11, CNTF, LIF, CLCF1 and CTF1 following various retinal insults [62,63,65-67]. In addition to increases from constitutive levels, OSM and IL-11 also exhibited stressor-dependent changes in expression. Specifically, OSM expression was greatest in young DBA/2 retina, suggesting that it may be induced early, in pre-degenerative states then return to lower levels with disease onset. Similarly, IL-11 expression was greatest in aged C57 retina, suggesting chronic elevation of this cytokine in aging. Interestingly, IOP-induced glaucoma attenuated age-related increases in IL-11 to levels consistent with retina in

predisposed to glaucoma, suggesting that the functional implications of IL-11 in aging and glaucomatous retina may differ. In the context of the gp130 data, normal aging induced complimentary increases in cytokine and gp130 expression, suggesting that elevated levels of IL-6 family cytokines result in increased signaling by these cytokines. In contrast, DBA/2 retina exhibited increased cytokine expression, but decreased gp130 expression, suggesting that, despite increases in cytokine levels, the ability of these cytokines to initiate signaling cascades is diminished. The same trend was noted with IL-6 signaling in DBA/2 mice, where expression of IL-6 receptor alpha was reduced, despite increases in IL-6 expression [19].

Overall, these data indicate that glaucoma-related stressors, including normal aging, genetic predisposition and IOP-induced glaucoma, differentially alter expression of the signal transducer gp130 and that these alterations have direct implications for astrocyte and Müller glia reactivity, RGC health and cytokine signaling. The utilization of the DBA/2J mouse model in this study limits its interpretation to long-term exposure to glaucomatous stressors. It is likely that gp130-mediated signaling by IL-6 family members also plays a role in more immediate responses to glaucomatous stressors, namely elevated IOP. As such, we are currently examining differences in the induction of gp130-mediated signaling via IL-6 family members in models of acute ocular hypertension.

Acknowledgements

The authors would like to thank the following individuals and centers for technical assistance with these studies: Dr. D'Anne Duncan (lab of Dr. Rebecca Sappington, Dr. Wendi Lambert (lab of Dr. David Calkins), and Karen Ho (lab of Dr. David Calkins) at the Vanderbilt Eye Institute, the Vanderbilt Cell Imaging Shared Resource Core (imaging), Jared LeBoeuf in the Vanderbilt Core Lab for Translational and Clinical Research (protein expression) and Latha Raju in the Vanderbilt University Medical Center Genome Sciences Resource Microarray Core (gene expression). We would also like to thank the Research Experience for High School Students program at the Vanderbilt's Center for Science Outreach for supporting author Michelle Won.

Grant Support

National Eye Institute Grant RO1EY020496 (RMS), National Eye Institute Core Grant P30EY08126 (Vanderbilt Vision Research Center), Research to Prevent Blindness-Career Development Award (RMS) and Initiative for Maximizing Student Diversity Grant 2R25GM62459-9 (Vanderbilt BRET; FDE).

References

1. Quigley HA (1999) Neuronal death in glaucoma. Prog Retin Eye Res 18: 39-57.
2. Nickells RW (2007) Ganglion cell death in glaucoma: from mice to men. Vet Ophthalmol 10 Suppl 1: 88-94.
3. Quigley HA, Broman AT (2006) The number of people with glaucoma worldwide in 2010 and 2020. Br J Ophthalmol 90: 262-267.
4. Nickells RW, Howell GR, Soto I, John SW (2012) Under pressure: cellular and molecular responses during glaucoma, a common neurodegeneration with axonopathy. Annu Rev Neurosci 35: 153-179.
5. Bosco A, Steele MR, Vetter ML (2011) Early microglia activation in a mouse model of chronic glaucoma. J Comp Neurol 519: 599-620.
6. Bosco A, Inman DM, Steele MR, Wu G, Soto I, et al. (2008) Reduced retina microglial activation and improved optic nerve integrity with minocycline treatment in the DBA/2J mouse model of glaucoma. Invest Ophthalmol Vis Sci 49: 1437-1446.
7. Brown GC, Neher JJ (2010) Inflammatory neurodegeneration and mechanisms of microglial killing of neurons. Mol Neurobiol 41: 242-247.
8. Hernandez MR, Miao H, Lukas T (2008) Astrocytes in glaucomatous optic neuropathy. Prog Brain Res 173: 353-373.
9. Langmann T (2007) Microglia activation in retinal degeneration. J Leukoc Biol 81: 1345-1351.
10. Morales I, Farías G, Maccioni RB (2010) Neuroimmunomodulation in the pathogenesis of Alzheimer's disease. Neuroimmunomodulation 17: 202-204.
11. Neufeld AH, Liu B (2003) Glaucomatous optic neuropathy: when glia misbehave. Neuroscientist 9: 485-495.
12. Sappington RM, Calkins DJ (2008) Contribution of TRPV1 to microglia-derived IL-6 and NFkappaB translocation with elevated hydrostatic pressure. Invest Ophthalmol Vis Sci 49: 3004-3017.
13. Tezel G, Wax MB (2003) Glial modulation of retinal ganglion cell death in glaucoma. J Glaucoma 12: 63-68.
14. Inman DM, Horner PJ (2007) Reactive nonproliferative gliosis predominates in a chronic mouse model of glaucoma. Glia 55: 942-953.
15. Sappington RM, Calkins DJ (2006) Pressure-induced regulation of IL-6 in retinal glial cells: involvement of the ubiquitin/proteasome pathway and NFkappaB. Invest Ophthalmol Vis Sci 47: 3860-3869.
16. Sappington RM, Chan M, Calkins DJ (2006) Interleukin-6 protects retinal ganglion cells from pressure-induced death. Invest Ophthalmol Vis Sci 47: 2932-2942.
17. Chidlow G, Wood JP, Ebneter A, Casson RJ (2012) Interleukin-6 is an efficacious marker of axonal transport disruption during experimental glaucoma and stimulates neuritogenesis in cultured retinal ganglion cells. Neurobiol Dis 48: 568-581.
18. Johnson EC, Morrison JC (2009) Friend or foe? Resolving the impact of glial responses in glaucoma. J Glaucoma 18: 341-353.
19. Sims SM, Holmgren L, Cathcart HM, Sappington RM (2012) Spatial regulation of interleukin-6 signaling in response to neurodegenerative stressors in the retina. Am J Neurodegener Dis 1: 168-179.
20. Knüpfer H, Preiss R (2008) sIL-6R: more than an agonist? Immunol Cell Biol 86: 87-91.
21. Taga T, Kishimoto T (1997) Gp130 and the interleukin-6 family of cytokines. Annu Rev Immunol 15: 797-819.
22. Rose-John S, Scheller J, Elson G, Jones SA (2006) Interleukin-6 biology is coordinated by membrane-bound and soluble receptors: role in inflammation and cancer. J Leukoc Biol 80: 227-236.
23. Hirano T, Ishihara K, Hibi M (2000) Roles of STAT3 in mediating the cell growth, differentiation and survival signals relayed through the IL-6 family of cytokine receptors. Oncogene 19: 2548-2556.
24. Heinrich PC, Behrmann I, Haan S, Hermanns HM, Müller-Newen G, et al. (2003) Principles of interleukin (IL)-6-type cytokine signalling and its regulation. Biochem J 374: 1-20.
25. Fang XX, Jiang XL, Han XH, Peng YP, Qiu YH (2013) Neuroprotection of interleukin-6 against NMDA-induced neurotoxicity is mediated by JAK/STAT3, MAPK/ERK, and PI3K/AKT signaling pathways. Cell Mol Neurobiol 33: 241-251.
26. Joos KM, Li C, Sappington RM (2010) Morphometric changes in the rat optic nerve following short-term intermittent elevations in intraocular pressure. Invest Ophthalmol Vis Sci 51: 6431-6440.
27. Sappington RM, Sidorova T, Long DJ, Calkins DJ (2009) TRPV1: contribution to retinal ganglion cell apoptosis and increased intracellular Ca2+ with exposure to hydrostatic pressure. Invest Ophthalmol Vis Sci 50: 717-728.
28. Chang B, Smith RS, Hawes NL, Anderson MG, Zabaleta A, et al. (1999) Interacting loci cause severe iris atrophy and glaucoma in DBA/2J mice. Nat Genet 21: 405-409.
29. Anderson MG, Smith RS, Hawes NL, Zabaleta A, Chang B, et al. (2002) Mutations in genes encoding melanosomal proteins cause pigmentary glaucoma in DBA/2J mice. Nat Genet 30: 81-85.
30. John SW, Smith RS, Savinova OV, Hawes NL, Chang B, et al. (1998) Essential iris atrophy, pigment dispersion, and glaucoma in DBA/2J mice. Invest Ophthalmol Vis Sci 39: 951-962.
31. Schraermeyer M, Schnichels S, Julien S, Heiduschka P, Bartz-Schmidt KU, et al. (2009) Ultrastructural analysis of the pigment dispersion syndrome in DBA/2J mice. Graefes Arch Clin Exp Ophthalmol 247: 1493-1504.
32. Narazaki M, Yasukawa K, Saito T, Ohsugi Y, Fukui H, et al. (1993) Soluble forms of the interleukin-6 signal-transducing receptor component gp130 in

human serum possessing a potential to inhibit signals through membrane-anchored gp130. Blood 82: 1120-1126.

33. Diamant M, Rieneck K, Mechti N, Zhang XG, Svenson M, et al. (1997) Cloning and expression of an alternatively spliced mRNA encoding a soluble form of the human interleukin-6 signal transducer gp130. FEBS Lett 412: 379-384.

34. Crish SD, Sappington RM, Inman DM, Horner PJ, Calkins DJ (2010) Distal axonopathy with structural persistence in glaucomatous neurodegeneration. Proc Natl Acad Sci U S A 107: 5196-5201.

35. Buckingham BP, Inman DM, Lambert W, Oglesby E, Calkins DJ, et al. (2008) Progressive ganglion cell degeneration precedes neuronal loss in a mouse model of glaucoma. J Neurosci 28: 2735-2744.

36. Bull ND, Guidi A, Goedert M, Martin KR, Spillantini MG (2012) Reduced axonal transport and increased excitotoxic retinal ganglion cell degeneration in mice transgenic for human mutant P301S tau. PLoS One 7: e34724.

37. Chang ML, Wu CH, Jiang-Shieh YF, Shieh JY, Wen CY (2007) Reactive changes of retinal astrocytes and Müller glial cells in kainate-induced neuroexcitotoxicity. J Anat 210: 54-65.

38. Lam TK, Chan WY, Kuang GB, Wei H, Shum AS, et al. (1995) Differential expression of glial fibrillary acidic protein (GFAP) in the retinae and visual cortices of rats with experimental renal hypertension. Neurosci Lett 198: 165-168.

39. Chen H, Weber AJ (2002) Expression of glial fibrillary acidic protein and glutamine synthetase by Muller cells after optic nerve damage and intravitreal application of brain-derived neurotrophic factor. Glia 38: 115-125.

40. Varela HJ, Hernandez MR (1997) Astrocyte responses in human optic nerve head with primary open-angle glaucoma. J Glaucoma 6: 303-313.

41. Gallego BI, Salazar JJ, de Hoz R, Rojas B, Ramírez AI, et al. (2012) IOP induces upregulation of GFAP and MHC-II and microglia reactivity in mice retina contralateral to experimental glaucoma. J Neuroinflammation 9: 92.

42. Woldemussie E, Wijono M, Ruiz G (2004) Müller cell response to laser-induced increase in intraocular pressure in rats. Glia 47: 109-119.

43. Shen F, Chen B, Danias J, Lee KC, Lee H, et al. (2004) Glutamate-induced glutamine synthetase expression in retinal Muller cells after short-term ocular hypertension in the rat. Invest Ophthalmol Vis Sci 45: 3107-3112.

44. Zhang S, Wang H, Lu Q, Qing G, Wang N, et al. (2009) Detection of early neuron degeneration and accompanying glial responses in the visual pathway in a rat model of acute intraocular hypertension. Brain Res 1303: 131-143.

45. Chidlow G, Holman MC, Wood JP, Casson RJ (2010) Spatiotemporal characterization of optic nerve degeneration after chronic hypoperfusion in the rat. Invest Ophthalmol Vis Sci 51: 1483-1497.

46. Chen KH, Wu CC, Roy S, Lee SM, Liu JH (1999) Increased interleukin-6 in aqueous humor of neovascular glaucoma. Invest Ophthalmol Vis Sci 40: 2627-2632.

47. Rhee KD, Yang XJ (2003) Expression of cytokine signal transduction components in the postnatal mouse retina. Mol Vis 9: 715-722.

48. Tanaka Y, Tanaka N, Saeki Y, Tanaka K, Murakami M, et al. (2008) c-Cbl-dependent monoubiquitination and lysosomal degradation of gp130. Mol Cell Biol 28: 4805-4818.

49. Lee HK, Seo IA, Shin YK, Park JW, Suh DJ, et al. (2009) Capsaicin inhibits the IL-6/STAT3 pathway by depleting intracellular gp130 pools through endoplasmic reticulum stress. Biochem Biophys Res Commun 382: 445-450.

50. Waetzig GH, Chalaris A, Rosenstiel P, Suthaus J, Holland C, et al. (2010) N-linked glycosylation is essential for the stability but not the signaling function of the interleukin-6 signal transducer glycoprotein 130. J Biol Chem 285: 1781-1789.

51. Inomata Y, Hirata A, Yonemura N, Koga T, Kido N, et al. (2003) Neuroprotective effects of interleukin-6 on NMDA-induced rat retinal damage. Biochem Biophys Res Commun 302: 226-232.

52. Tezel G, Chauhan BC, LeBlanc RP, Wax MB (2003) Immunohistochemical assessment of the glial mitogen-activated protein kinase activation in glaucoma. Invest Ophthalmol Vis Sci 44: 3025-3033.

53. Grieshaber MC, Orgul S, Schoetzau A, Flammer J (2007) Relationship between retinal glial cell activation in glaucoma and vascular dysregulation. J Glaucoma 16: 215-219.

54. Tezel G, Yang X, Luo C, Peng Y, Sun SL, et al. (2007) Mechanisms of immune system activation in glaucoma: oxidative stress-stimulated antigen presentation by the retina and optic nerve head glia. Invest Ophthalmol Vis Sci 48: 705-714.

55. Lye-Barthel M, Sun D, Jakobs TC (2013) Morphology of astrocytes in a glaucomatous optic nerve. Invest Ophthalmol Vis Sci 54: 909-917.

56. Ebneter A, Casson RJ, Wood JP, Chidlow G (2010) Microglial activation in the visual pathway in experimental glaucoma: spatiotemporal characterization and correlation with axonal injury. Invest Ophthalmol Vis Sci 51: 6448-6460.

57. Yoshida N, Ikeda Y, Notomi S, Ishikawa K, Murakami Y, et al. (2013) Laboratory evidence of sustained chronic inflammatory reaction in retinitis pigmentosa. Ophthalmology 120: e5-12.

58. Zhao TT, Tian CY, Yin ZQ (2010) Activation of Müller cells occurs during retinal degeneration in RCS rats. Adv Exp Med Biol 664: 575-583.

59. Fukushima M, Setoguchi T, Komiya S, Tanihara H, Taga T (2009) Retinal astrocyte differentiation mediated by leukemia inhibitory factor in cooperation with bone morphogenetic protein 2. Int J Dev Neurosci 27: 685-690.

60. Ueki Y, Le YZ, Chollangi S, Muller W, Ash JD (2009) Preconditioning-induced protection of photoreceptors requires activation of the signal-transducing receptor gp130 in photoreceptors. Proc Natl Acad Sci U S A 106: 21389-21394.

61. Kirsch M, Trautmann N, Ernst M, Hofmann HD (2010) Involvement of gp130-associated cytokine signaling in Müller cell activation following optic nerve lesion. Glia 58: 768-779.

62. Johnson EC, Doser TA, Cepurna WO, Dyck JA, Jia L, et al. (2011) Cell proliferation and interleukin-6-type cytokine signaling are implicated by gene expression responses in early optic nerve head injury in rat glaucoma. Invest Ophthalmol Vis Sci 52: 504-518.

63. Vázquez-Chona F, Song BK, Geisert EE Jr (2004) Temporal changes in gene expression after injury in the rat retina. Invest Ophthalmol Vis Sci 45: 2737-2746.

64. Schuettauf F, Zurakowski D, Quinto K, Varde MA, Besch D, et al. (2005) Neuroprotective effects of cardiotrophin-like cytokine on retinal ganglion cells. Graefes Arch Clin Exp Ophthalmol 243: 1036-1042.

65. Wu Q, Zhang M, Song BW, Lu B, Hu P (2007) Expression of ciliary neurotrophic factor after induction of ocular hypertension in the retina of rats. Chin Med J (Engl) 120: 1825-1829.

66. Chu Q, Zhang J, Wu Y, Zhang Y, Xu G, et al. (2011) Differential gene expression pattern of diabetic rat retinas after intravitreal injection of erythropoietin. Clin Experiment Ophthalmol 39: 142-151.

67. Song Y, Zhao L, Tao W, Laties AM, Luo Z, et al. (2003) Photoreceptor protection by cardiotrophin-1 in transgenic rats with the rhodopsin mutation s334ter. Invest Ophthalmol Vis Sci 44: 4069-4075.